# Experimental and Numerical Study of a Supercritical Wing Performance at Low Reynolds Numbers Equipped with Different Winglet Planforms

Parisa Ghanooni [1], Mostafa Kazemi [1], Meisam Heydari [2], Mahmoud Mani [1]*

[1] Department of Aerospace Engineering, Amirkabir University of Technology, Tehran, Iran
[2] Department of Mechanical Engineering, Polytechnic of Milan, Milan, Italy

**ABSTRACT:** In the era of rapid technological developments, the green aircraft and winglets of airplanes play a crucial role in reducing fuel consumption and its ensuing pollution. In this regard, the novelty of this paper is to focus on investigating the effect of the different geometrical parameters of winglets planforms on improving the aerodynamic performance of a wing with a supercritical airfoil (NACA 641412) at lower Reynolds numbers (take-off and landing phase). These investigations were conducted experimentally in a wind tunnel by force measurements through an external force balance. The aerodynamic coefficients of CL and CL/CD were obtained for the clean wing and nine various winglet planforms at a wide range of angles of attack from -4° to 20° and Reynolds numbers from Re=0.99×105 to Re=1.98×105. Furthermore, to get better insight into the physics of the flow, the numerical simulation of specific cases was carried out. According to the force measurement and vorticity magnitude results, among single winglets of W1, W2, W3, and W4, the W1 winglet with vertical height and linear side showed a better performance in all Reynolds numbers with a maximum lift increment of 26%; also, the W7 winglet planform represented the best performance as in double winglets with a maximum lift-to-drag ratio increment of 40%.

## 1- Introduction

Over the past 50 years, global warming has been the main concern of engineers in various fields. Admittedly, fuel consumption and its ensuing CO2 pollution is the most important element to be considered, and according to the statistics, the aviation industry produces 2% of CO2 emissions in the transportation sector [1]. Consequently, aerodynamic performance improvement is of vital importance for aerospace engineers to meet the high-level climate action goals of achieving the annual 1.5% fuel efficiency improvement [2].

One of the ways to enhance the aerodynamic performance is reducing the drag force which is divided into profile drag and drag due to lift for a conventional subsonic airplane. In this regard, the main parameter affecting the fuel efficiency and performance of the wing of an airplane is lift-induced drag reduction, which is generated from wing tip vortices [3]. It is worthwhile to mention that, wingtip vortices can be hazardous in some cases, due to their long durability in the air that can cause serious problems for other incoming airplanes; thus, the aviation industry is forced to determine adequate distances between aircrafts, which can financially be disadvantageous. Therefore, there have been a lot of significant efforts to develop technologies for decreasing the drag due to lift and avoiding vortex formation, such as winglets, wingtip devices, and classical theories, including

higher $AR^1$ and elliptical load distribution [4]. The structural considerations and increased frictional drag due to higher AR wings confine the use of classical methods for reducing the induced drag. Therefore, in recent years, winglets have been focused on controlling the drag due to the lift of conventional airplanes.

As previously mentioned, part of the total drag of an airplane is assigned to the drag due to the lift called induced drag. Theoretically, the major difference between the physics of the flow around a 2D and a finite wing is the flow structures near the tip of the wing. The pressure difference between the lower and upper surface of the wing, not only generates the lift force but also creates a downward velocity component called downwash at the tip of the wing, which makes the lift force have a component in the opposite direction of the flow that leads to a drag force introduced as induced drag. By shedding this downwash flow to the wake of the wing, wingtip vortices can be generated, as presented in Fig. 1 Clearly, by preventing the construction of these vortices, induced drag can be reduced, and this concept was first become practical by Richard Whitcomb at NASA's Langley research center in 1976 by adding winglets to a narrow-body jet transport wing [5]. Indeed, the role of the winglet is to make wingtip vortices breakdown and dissipate, and accordingly, reduce their size and strength by preventing the leakage of the flow from the
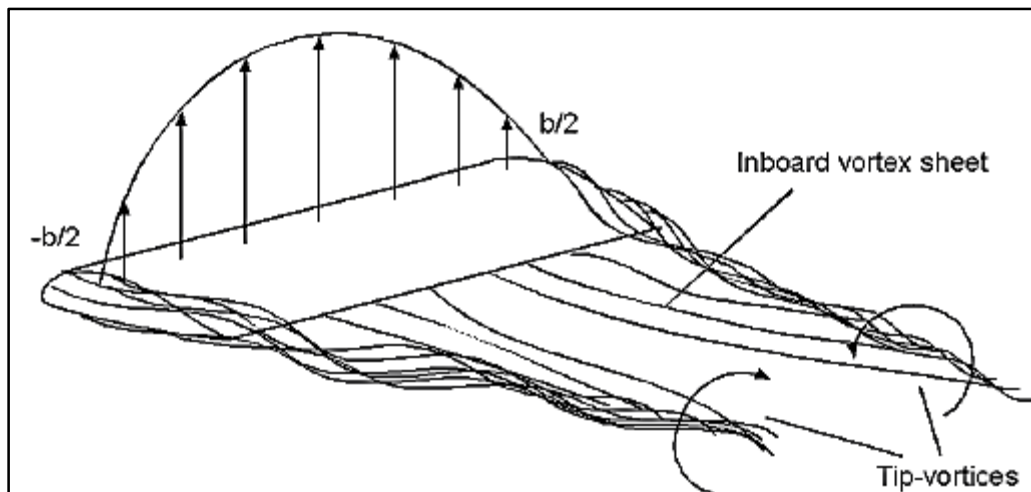
**Fig. 1. Formation of Wingtip Vortices [6]**

lower surface to the upper surface.

Since the winglet was introduced by Richard Whitcomb, there have been various experimental [6-8] and numerical investigations [9, 10] related to the impact of winglets on wingtip vortices and induced drag reduction as well as research for optimized winglet design approaches [10-24]. It is worthwhile to mention that this concept of winglet introduced by Whitcomb had many applications in industry, such as wind turbines [23, 24] heat exchangers [25], turbomachinery [26], etc. in addition to the ones that are just attached to the wings. However, according to the main purpose of this paper, the literature focuses on the application of winglets in aviation and commercial airplanes. For instance, Montaya et al [27] through experimental measurements of four different configurations concluded that aerodynamic gain to structural weight penalty is more in the case of winglets compared to wing extensions.

In addition, as time passed, new and novel shapes of winglets were presented throughout the entire world. One of these types was spiroid-type winglets that were patented by Gratzar in 1992 [28]. He claimed that this type of winglet represented a better performance and could eliminate wingtip vortices, completely. One of the most significant studies carried out by researchers is Keizo Takenaka et al's work [29], in which he conducted a multidisciplinary optimization focusing on designing an optimized winglet for a commercial jet aircraft. With the help of computational fluid dynamics, finite element-based weight calculations, and multi-objective genetic algorithms; he finally concluded that winglet cant angle and span length are dominant parameters for controlling drag reduction. Also, considering different winglet angles, T. Seshaiah et al [10] have also conducted a numerical study of different winglet configurations to achieve better performance. Through this study, they concluded that winglets

with variable angles can be a feasible recommendation for aircraft performance improvement. Indeed, according to the results obtained from Toor et al's [30] study through computational methods, the effectiveness of winglets has an inverse relation with its cant angle; in other words, winglets attached to the wing at lower cant angles represent better performance. Also, about other parameters such as toe angle and taper ratio, it is found that there is an optimum value until which the efficiency increases and then decreases.

Apart from the efforts for designing efficient winglets and assessing the effectiveness of different methods for predicting the airfoil coefficients, many researchers have focused on the effect of the winglet on the flow field of the wing and wingtip vortices physics. Sohn and Chang [31] studied the wingtip vortical structures of three wingtip configurations at different velocities and angles of attack through smoke-wire visualization along with particle image velocimetry. The results of this research have shown that the winglet can reduce the strength of these wingtip vortices and move them upward and outboard. Furthermore, in 2016, Narayan and John investigated [16] the effect of the three different winglet designs in improving the efficiency of the clean wing numerically using the CFD method. According to the results of this paper, the multi-tipped winglet with four tips is considered the most efficient design. Also, another research conducted by Ilie et al in 2019 [32] explored the effect of the double-winglets in comparison with the single-winglet with the LES approach, and it was concluded that the double-winglet configuration has a better performance.

Over the past five decades, many researchers around the globe have presented an optimized winglet design that may be claimed to have superior performance. Although winglet geometrical parameters investigation has been studied in the field of wind turbines by Mourad et al [33]. Through this

**Table 1. Wind tunnel experiments parameters**

| | |
|---|---|
| Models | NACA 641412 Wing, Four Single Winglets, Five Double Winglets |
| Free Stream Velocities | 10, 15, and 20 m/s |
| Angles of Attack | -4°, -2°, 0, ..., 20° |

study, they investigated the effect of winglet height (H) and toe angle ($\alpha_w$) on the turbine performance numerically using the CFD approach to obtain the optimum value of these two parameters.

Through the literature, some significant and relevant work has been described; however, it could not be found any studies conducted investigating the effect of planform geometrical parameters on winglet efficiency in the case of a supercritical wing performance enhancement at lower Reynolds numbers (take-off and landing phase of flight), which is a regime at which these types of airfoils do not show a good performance. It is acceptable that having a curved or straight edge and having an inclined or vertical height edge for winglet planforms affect the performance of a wing equipped with a winglet. Therefore, the effect of these various geometrical parameters has been discussed in this paper. In addition, it is worthwhile to mention that the major consumer of winglets in aviation is the general transport jets, which fly in a transonic regime and are designed to use the winglets for the climb and descent phases of the flight to enhance the lift force at take-off and landing. Utilizing winglets at these two phases helps the aircraft to have both short take-off /landing distance (STOL[1]) and lower touch-down/rotation speed. Therefore, by taking all the above-mentioned arguments into discussion, this paper aims to analyze the flow over a rectangular supercritical wing equipped with winglets at low Reynolds numbers, experimentally and numerically. For this purpose, several wind tunnel experiments and numerical simulations are carried out for a number of winglets with diverse geometrical parameters to meet the objective of fundamentally studying wingtip vortice behavior and its effect on the aerodynamic performance of the tested supercritical wing. Thus, the interesting innovation of this study is the extensive study investigation of winglet planform shape parameters effects on a supercritical airfoil at take-off/landing phases. In the subsequent sections, the experimental setup and computation setup will be explained, then the results obtained from this study in terms of lift coefficient, drag coefficient, lift-to-drag ratio, drag polar, and wingtip vortices distribution will be analyzed thoroughly and comparatively for different cases.

---

1  Short Take Off Landing

## 2- Experimental Methodology and Numerical Setup

In this section, the shapes of the designed winglets will be illustrated. Furthermore, the wind tunnel experimental and computational setup will be explained.

The accurate and extensive analysis of different flight conditions of an aircraft requires the tests to be conducted over a wide range of chord-based Reynolds numbers and angles of attack. The test plan of all the tests carried out in this research is tabulated in Table 1. It is shown that the free stream velocities of 10 m/s, 15 m/s, and 20 m/s corresponding to the chord-based Reynolds numbers of Re = $0.99 \times 10^5$, Re = $1.48 \times 10^5$, and Re = $1.98 \times 10^5$ were chosen during the tests; besides, the experiments were carried out in the angles of attack ranging from -4° to 20°.

### 2- 1- Model and Winglet Planforms

For investigating the effect of different geometrical parameters on the aerodynamic performance of NACA $64_{(1)}412$ wing, the planforms shown in Fig.2, considering the fact that being curved or straight for winglet planform edges and being inclined or vertical for the height of the winglet affect the performance of the wing equipped with a winglet were designed with the help of CATIA software and manufactured using Plexi Glass material and Laser-Cutting method. For these winglets, the height is 100 mm and their chord is the same as the base wing. (150 mm). These nine winglets are divided into two groups of single and double winglets. In the single-winglet group, the four winglets differ from each other in terms of curved or linear frontal edge (W1 and W3 & W2 and W4) and slanted or vertical height edge (W1 and W2 & W3 and W4). Also, in the second double-winglet group, the winglets from W5 to W8 are a double form of the single winglets of W1 to W4. At last, the W9 winglet is a combination of all these geometrical considerations.

### 2- 2- Wind Tunnel and Force Measurement Setup

The aerodynamic force measurements were conducted in the low-speed open-circuit wind tunnel with a rectangular test section of $1 \times 1 \times 1.8$ m³, contraction ratio of 9:1, and turbulence level as low as 0.1% at DANA Aerodynamic Laboratory at Amirkabir University of Technology. The schematic of the test set-up and all the facilities related to these measurements is shown in Fig. 3 . The aerodynamic forces of the lift (*L*) and
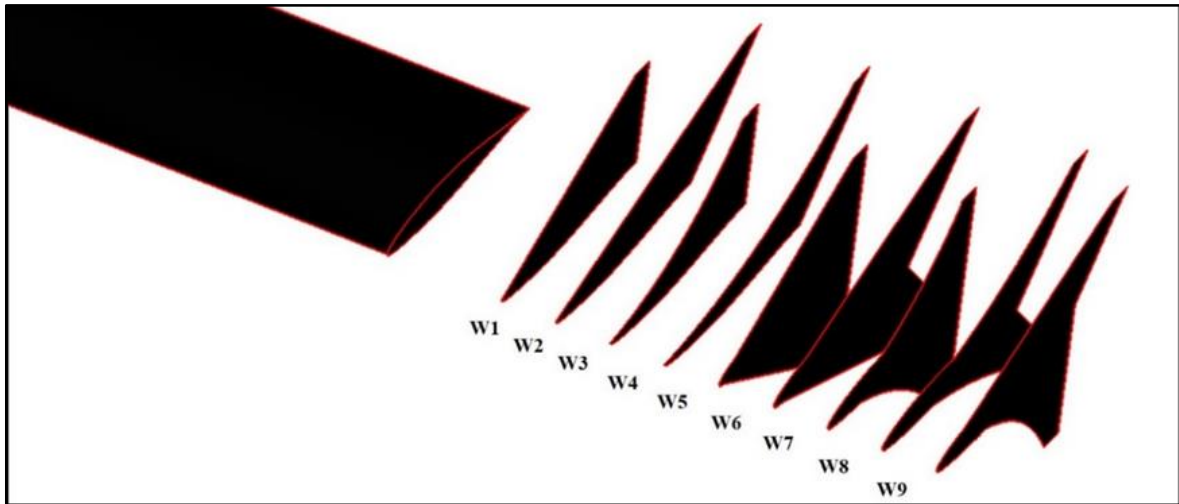
**Fig. 2. NACA 641412 wing accompanied by nine different winglets**
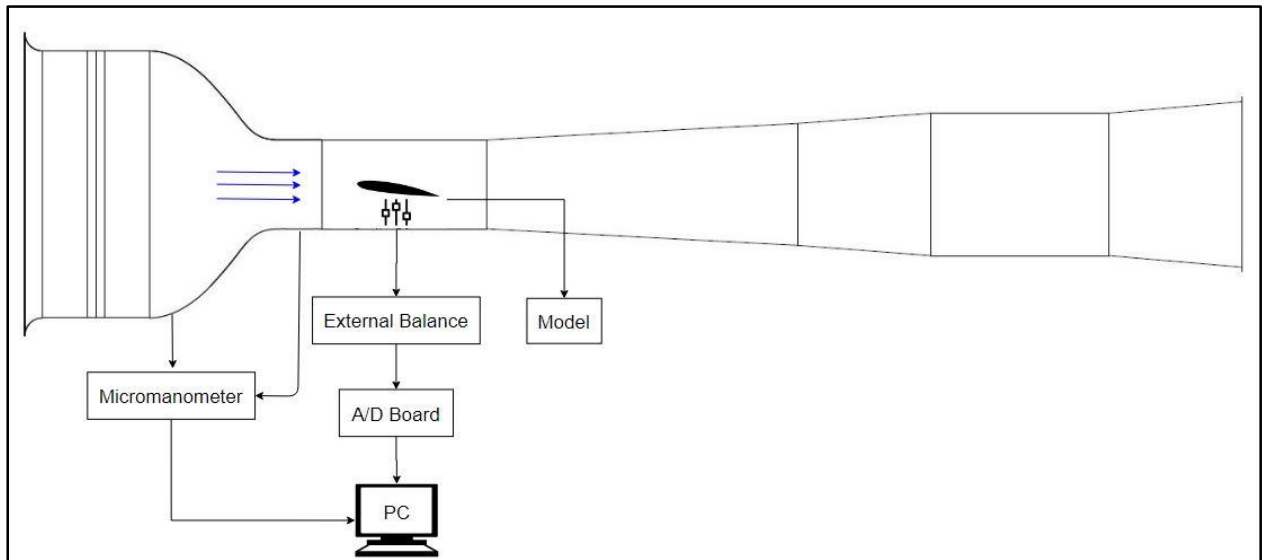


**Fig. 3. Schematic of balance force measurement set-up**

drag (*D*) were measured using an external three-component balance manufactured by TecQuipment attached to the vertical wall of the wind tunnel test section. The forces acting on the model are transmitted by cables to three strain-gauged load cells with a capacity of 10 kg for the Lift component and 5 kg for the Drag component and a combined full-scale error of less than 3 g. Also, the diameter of the model strut should be 12 mm. Load cell calibration and correction of the blockage effect on the force measurement have been conducted according to [34]. As such, A Honeywell pressure sensor with a maximum range of 5 mbar and 0.1% FS error was used to measure the wind tunnel velocity. With respect to the mentioned error values and considering Equation (1), ±0.000294 would be obtained for calculating the force coefficients. Also, a maximum of ±0.001 difference in the value of measured force coefficients was observed in test repetition which is higher than the calculated error. Thus, it can be concluded that all values for force coefficients in this paper have ± 0.001 error bar which is neglected to show in the following figures due to better understanding.

$$C_F = \frac{F}{\frac{1}{2}\rho V^2 S} = \frac{F}{(P_{SC} - P_{TS})S} \qquad (1)$$

## 2- 3- Numerical methodology
### 2- 3- 1- Governing Equations and numerical scheme
Numerical simulation of the flow field around the baseline supercritical wing, wing equipped with the W1 winglet planform model, and wing equipped with W7 winglet planform has been carried out using commercial CFD software. The solution of the present case is solved by a steady Reynolds Averaged three-dimensional Navier-Stokes equations equation. The following mathematical formulations [35] are solved for the current study:

Continuity:

$$\frac{\partial u}{\partial x} + \frac{\partial v}{\partial y} + \frac{\partial w}{\partial z} = 0 \qquad (2)$$

Momentum:

$$u\frac{\partial u}{\partial x} + v\frac{\partial u}{\partial y} + w\frac{\partial u}{\partial z} =$$
$$-\frac{1}{\rho}\frac{\partial p}{\partial x} + \nu(\frac{\partial^2 u}{\partial x^2} + \frac{\partial^2 u}{\partial y^2} + \frac{\partial^2 u}{\partial z^2}) \qquad (3)$$

$$u\frac{\partial v}{\partial x} + v\frac{\partial v}{\partial y} + w\frac{\partial v}{\partial z} =$$
$$-\frac{1}{\rho}\frac{\partial p}{\partial y} + \nu(\frac{\partial^2 v}{\partial x^2} + \frac{\partial^2 v}{\partial y^2} + \frac{\partial^2 v}{\partial z^2}) \qquad (4)$$

$$u\frac{\partial w}{\partial x} + v\frac{\partial w}{\partial y} + w\frac{\partial w}{\partial z} =$$
$$-\frac{1}{\rho}\frac{\partial p}{\partial z} + \nu(\frac{\partial^2 w}{\partial x^2} + \frac{\partial^2 w}{\partial y^2} + \frac{\partial^2 w}{\partial z^2}) \qquad (5)$$

Where u, v, and w are the velocity components, p pressure, ρ density, and ν is kinematic viscosity.

There are various turbulence models for solving RANS equations, including Spalart Allmaras, k-ε, and K-ω SST. Thus, according to the [16], among these turbulence models, the two-equation turbulence model of k-ω SST is considered for the present study. This model was first developed by Menter [35] to integrate the K-ω turbulence model with higher capabilities for near-wall flow physic simulation and the K-ε turbulence model for the flow far from the wall that has acceptable accuracy for aerodynamic applications with adverse pressure gradient and separation predictability. The SIMPLE algorithm is used to calculate the coupling between the pressure and velocity fields. The second-order accurate upwind scheme in the spatial domain is adopted in simulations because of its stability and accuracy based on previous studies.

### 2- 3- 2- Computational Domain and Boundary Conditions
For accurate simulation and based on the domain study, the considered domain for simulation is 40×20×15 times bigger than the model chord length. Velocity Inlet boundary conditions for air inlet to the domain, Pressure Outlet by zero-gauge pressure for the outlet, and Symmetry for other sides are selected for boundary conditions based on previous studies and experiences. Also, the wing surface is treated as a stationary wall with the no-slip condition. Fig. 4 shows the computational domain and selected boundary conditions schematically.

### 2- 3- 3- Grid generation and mesh independency
The ICEM CFD Hexagonal grid is selected for mesh generation of the previously described air domain. The number of total elements is chosen based on the mesh independence study for accurate analysis and less computational cost. Variation of the Drag coefficient versus the number of grids is shown in Fig. 5 which is the number of 3.3 million cells selected for the final grid which has a suitable computational cost and enough precision. The final grid picture from the side view is presented in Fig. 6 and Table 2. The mesh consists of a 10-layer "Boundary Layer" mesh with a first layer height of 2.5×10⁻⁵ m to guarantee a Y+ value lower than 1 and 1.2 ratio for height increment. Also, the number of nodes on the surface of the wing is considered based on the control of the AR value lower than 20 in the whole of the wing surface.

### 2- 3- 4- Numerical validation
For validating the numerical scheme used in the current study for simulation of the flow field around a supercritical wing equipped with a winglet, experimental results of the present case at the velocity of V=10 m/s condition are
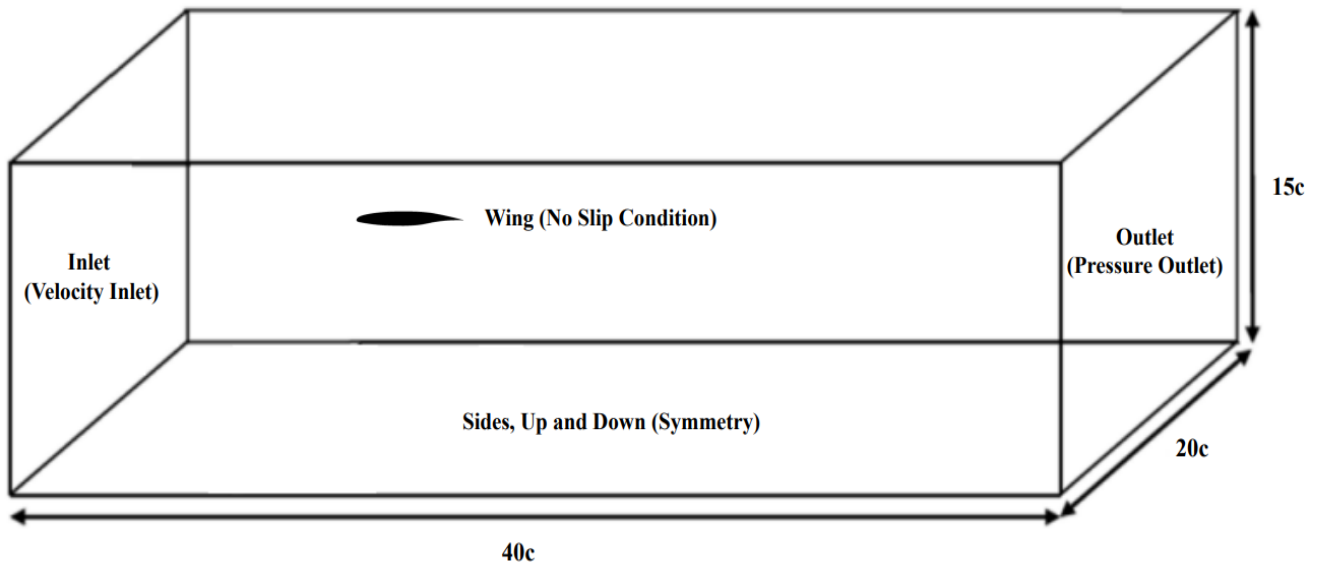
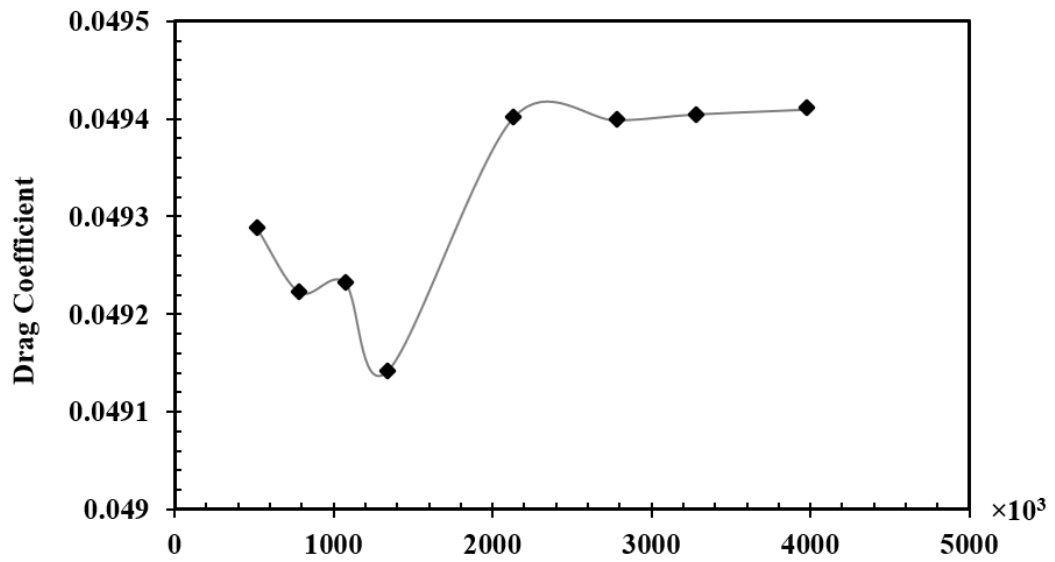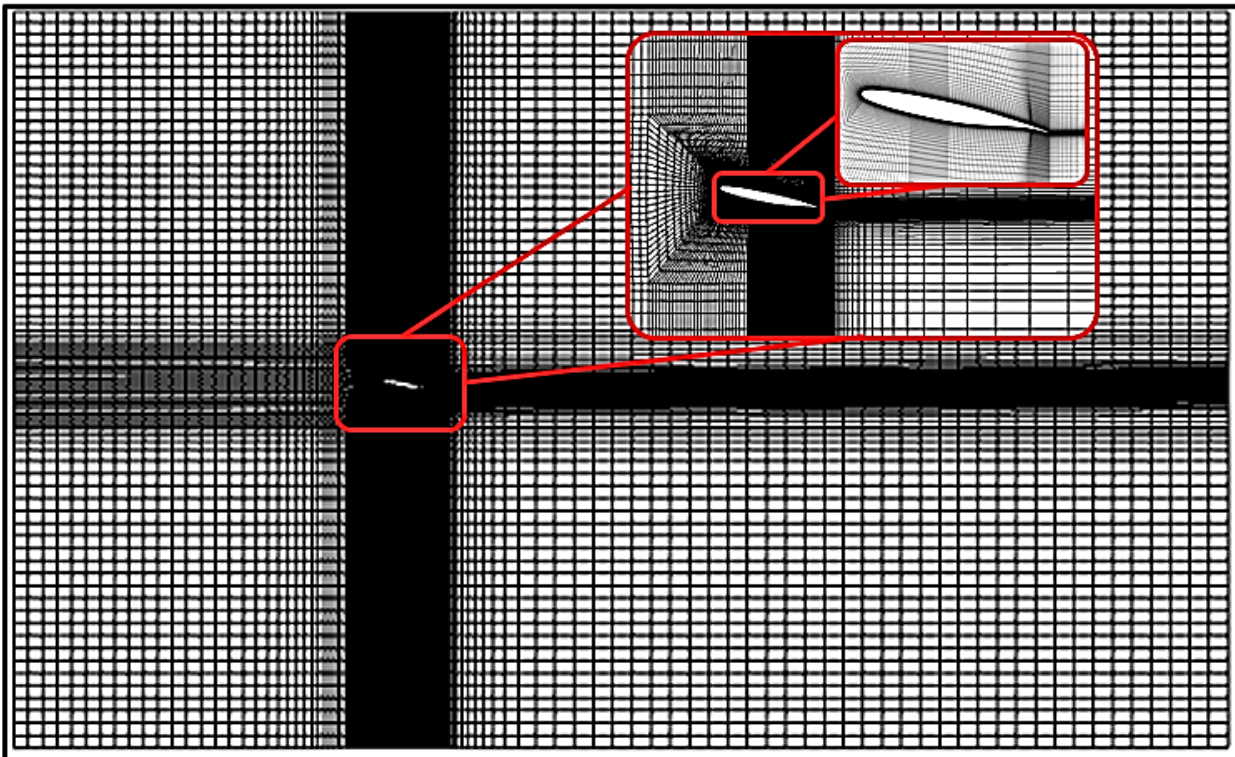**Fig. 4. Schematic of the computational domain and boundary conditions**

**Fig. 3. Schematic of balance force measurement set-up**

**Table 2. Percent comparison of mesh independency analysis**

| No. of Cells (×10³) | Drag Coefficient | Variation (%) |
|---|---|---|
| 500 | 0.04928 | 0.000 |
| 800 | 0.04922 | 0.120 |
| 1100 | 0.04923 | 0.020 |
| 1300 | 0.04914 | 0.018 |
| 2100 | 0.0494 | 0.053 |
| 2800 | 0.0494 | 0.000 |
| 3300 | 0.049405 | 0.010 |
| 4000 | 0.049401 | 0.008 |



**Fig. 6.Grid of the symmetry plane and boundary layer mesh**
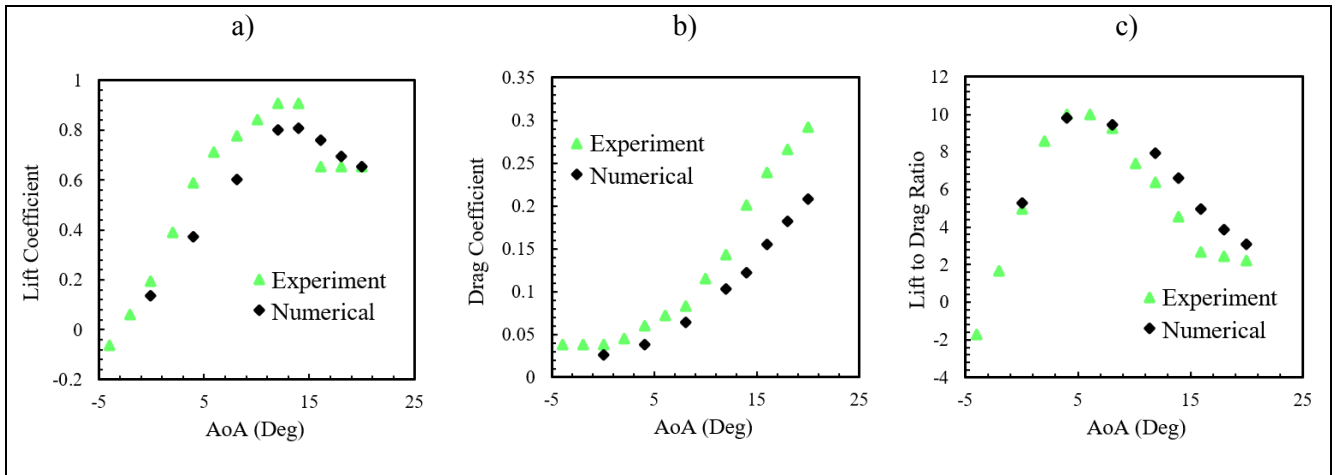
**Fig. 7. Comparison of Lift coefficient, drag coefficient, and Lift to Drag ratio of the wing with W1 wing-let analyzed experimentally and numerically in this study**

**Table 3. Comparison of experimental and numerical results**

| | Lift Coefficient | | | Drag Coefficient | | |
|---|---|---|---|---|---|---|
| *AOA* (deg) | *$CL_E$* | *$CL_N$* | *Error* | *$CD_E$* | *$CD_N$* | *Error* |
| 0 | 0.185 | 0.154 | 0.167 | 0.031 | 0.025 | 0.193 |
| 4 | 0.382 | 0.372 | 0.027 | 0.041 | 0.038 | 0.073 |
| 8 | 0.591 | 0.606 | 0.025 | 0.059 | 0.064 | 0.078 |
| 12 | 0.721 | 0.802 | 0.100 | 0.081 | 0.101 | 0.198 |

used for comparing CFD calculated lift coefficient, drag coefficient, and Lift to Drag ratio. Fig. 7a) displays the lift coefficient of the tested wing case versus the values obtained from numerical simulation representing a difference of less than 5%, which confirms the validity of this numerical scheme. The major difference between the two methods is in the stall area, which is due to the lack of CFD's ability to model the flow with high velocity and pressure gradient in the separation region. According to the experimental results, the wing stalls suddenly at AoA = 14°, but the CFD method presents a slight stall. It is worthwhile to mention that, for the other flow phenomena, both methods confirm each other.

The comparison of the experimental and numerical results of the CD is represented in Fig. 7. b that the difference between the two methods at lower angles of attack (lower than 12°) is less than 2 percent and by increasing the angle of attack, the difference is going to grow. Also, the L/D plot of two different CFD and Wind tunnel methods, which are shown in Fig. 7c has a good agreement due to differences lower than 3.5% at all angles of attack.

Also, for better verification of the results obtained from numerical simulations, Table 3 is provided to show the difference percentage between numerical and experimental results.

# 3- Results and Discussion

Results of the previously mentioned experiments for winglet-equipped wings at different angles of attack and three different free stream velocities are presented in this section. First, the effect of various single-winglet planforms on aerodynamic parameters of the supercritical wing, including $CL$ and $CL/CD$ will be explained. In the second section, the effect of different double winglets will be analyzed on the aerodynamic coefficients of the supercritical wing. In addition, the CFD approach was used to get better insight into the physics of the flow by contours of the vorticity field for the winglet planforms responsible for the most lift coefficient increment (W1) and maximum lift-to-drag ratio (W2).

## 3- 1- Single Winglet Planforms

The results of the lift coefficient obtained for the NACA $64_1412$ wing equipped with various single winglet planforms (W1-W4, see Fig. 8) at $Re_c = 0.99 \times 10^5$, $Re = 1.48 \times 10^5$, and $Re = 1.98 \times 10^5$ will be discussed in the subsequent paragraphs.

Fig. 8 shows that the lift coefficient of the clean wing increases in a semi-linear trend up to 14°, at which the wing stalls. It should be noted that this wing represents a positive lift coefficient even at zero degree angle of attack due to its cambered nature ($CL_{\alpha = 0} > 0$). According to the results, all single-winglet planforms have the same effect on the aerodynamic characteristics of the NACA $64_1412$ wing, including the $CL_{max}$, $CL_{\alpha=0}$, $CL_\alpha$, and stall behavior. All winglets increased the $CL_{max}$, $CL_{\alpha = 0}$, and $CL_\alpha$, whereas the stall angle of the wing does not vary by implying single-winglet for different free stream Reynolds numbers. ($\alpha_{stall} = 14°$). These phenomena indicate that adding winglet help the flow field around the wing become more 2D by controlling the wingtip vortices which leads to higher aerodynamic parameters, such as $CL_{max}$, $CL_\alpha = 0$, and $CL_\alpha$, for the wing with winglets.

Furthermore, by analyzing the lift coefficient of single winglet planforms comparatively, it can be deduced that the slanted (W2) or curved edge (W3) characteristics related to the winglet planform, did not show a better performance. Unlike the W1 winglet that offers the most increment of lift coefficient, it can be inferred from the results that the combined winglet of W4 (both slanted and curved edge) represented the least lift coefficient increment at $Re = 0.99 \times 10^5$, and among all these four various winglet planforms, W2 planform is the second-best winglet. These results are also valid for the higher Reynolds numbers of $Re = 1.48 \times 10^5$ and $Re = 1.98 \times 10^5$; however, the value of increment of aerodynamic characteristics due to the winglet planforms is reduced as the Reynolds number increases.

By taking all the above-mentioned arguments into account, it can be indicated that the wingtip vortex caused by the pressure difference at the tip of the wing implies a downward velocity component named downwash leading to a reduction in the angle of attack. According to the results, the wings equipped with winglets showed a higher lift coefficient due to canceling the effect of downwash. Also, among all these single planforms of winglets, the W1 Winglet represented the best performance at all low Reynolds numbers.

Furthermore, the L/D ratio is an essential parameter to be analyzed for different winglet planforms. Fig. 6 shows the L/D ratio as a function of the angle of attack for six configurations. As shown in this figure, there is no difference between the angle of attack, at which maximum $CL/CD$ occurs for both the clean wing equipped with a winglet and the baseline wing. Also, by comparing the $CL/CD$ diagram for different winglets, it can be inferred that the W1 winglet showed a better performance compared to the clean wing up to 4°; afterward, the $CL/CD$ of this winglet is lower than the base wing. However, the $CL/CD$ diagram related to the W2 winglet became lower than the clean wing at a lower angle of attack compared to the W1 winglet. Also, W3 and W4 showed the same behavior as the W2 winglet. Therefore, the W1 winglet represented the most $CL/CD$ increment among other single winglet planforms.
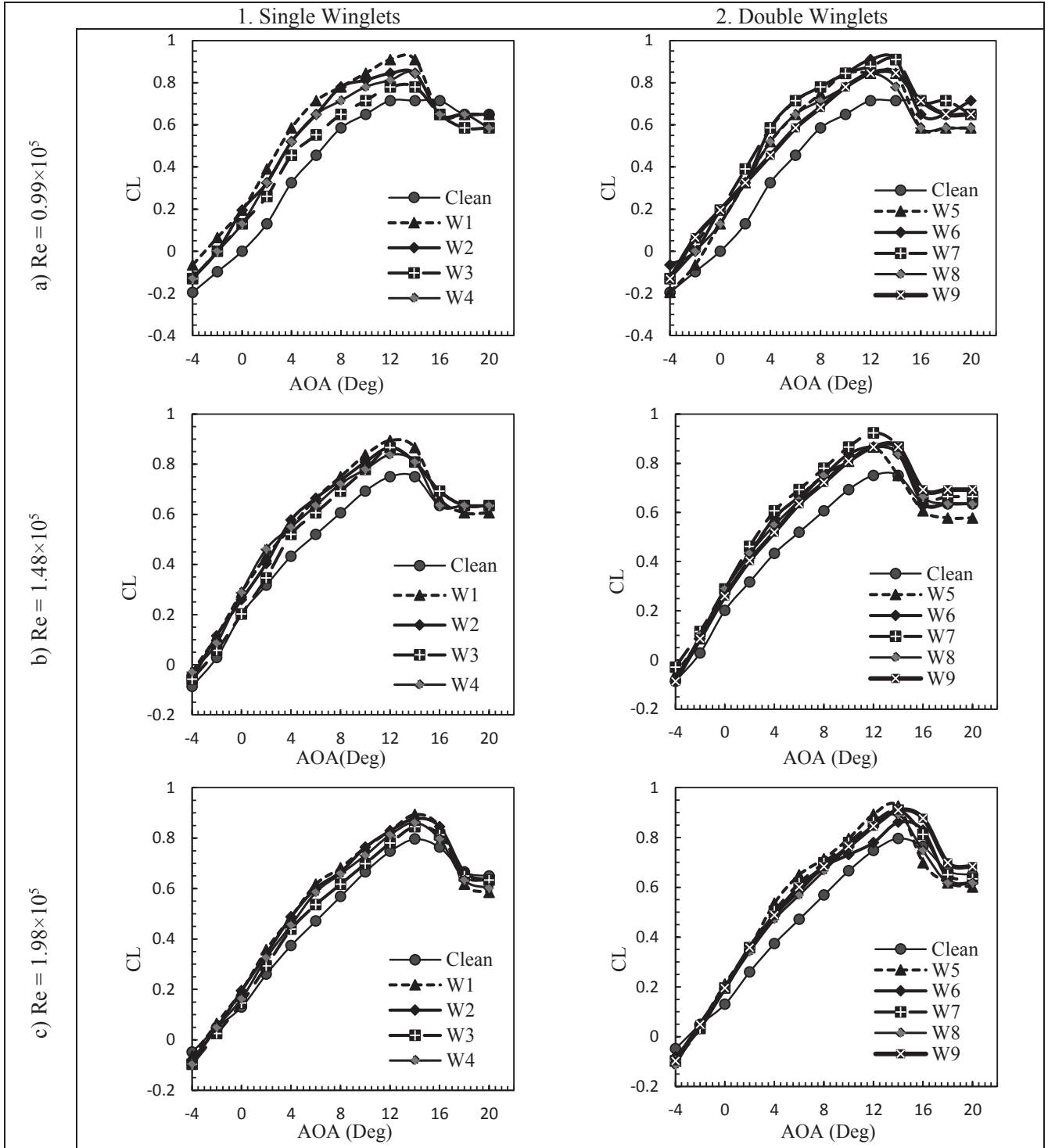
## 3- 2- Double Winglet Planforms

As illustrated in Fig. 8, the W7 and W6 winglets increased the lift coefficient of the NACA $64_1412$ wing substantially. By comparing double winglets with their single forms at the same Reynolds number, it can be concluded that using the double form of the winglets is better than the single form from the lift coefficient increment point of view except for the W1 singlet winglet planform that increased the lift coefficient more than its double form.

In the case of the clean wing with double winglets, generally, for both the base wing and the wing equipped with winglet W5, the angle of the maximum $CL/CD$ is 6° and their behavior is the same. First, for both wings, $CL/CD$ increased up to 6°, and then decreased. W5 winglet showed a lower lift-to-drag ratio relative to the clean wing at lower angles of attack less than 4°. W6 is the same as W5, but at negative angles of attack, it showed a better performance after the W9 winglet which increased the $CL/CD$ substantially. Among all these winglets, the W7 winglet represented the best performance by improving the $CL/CD$ ratio at lower angles up to almost 5°. Also, W8 is the second-best winglet for improving the $CL/CD$ ratio.

At $Re = 1.48 \times 10^5$, the angle of maximum $CL/CD$ ratio for all winglets and clean wing decreased from 6° to 4°. Also, the performance of the wing was reduced at lower angles of attack by increasing the Reynolds number. Admittedly, as illustrated in Fig. 9, the W7 winglet improved the performance of the wing at this Reynolds number at all angles of attack. In contrast, other winglets did not show any improvement in $CL/CD$.

In the following, for double winglets, W7 increased the $CL/CD$ and the AOA maximum substantially in comparison with other winglets. Also, W6, W8, W9, and W5 winglets increased the $CL/CD$ before they reached the $AOA_{maximum}$. It should be noted that W8 is the second best, and the W9 winglet is the worst winglet in this Reynolds number. By increasing the velocity from 10 m/s to 15 m/s, the $CL/CD$ diagram related to the W1 and W4 winglet showed a better performance compared to the clean wing at all angles of

**Fig. 8. Lift coefficient versus angle of attack for wing with different winglets at different Reynolds numbers in two winglet planforms categories**
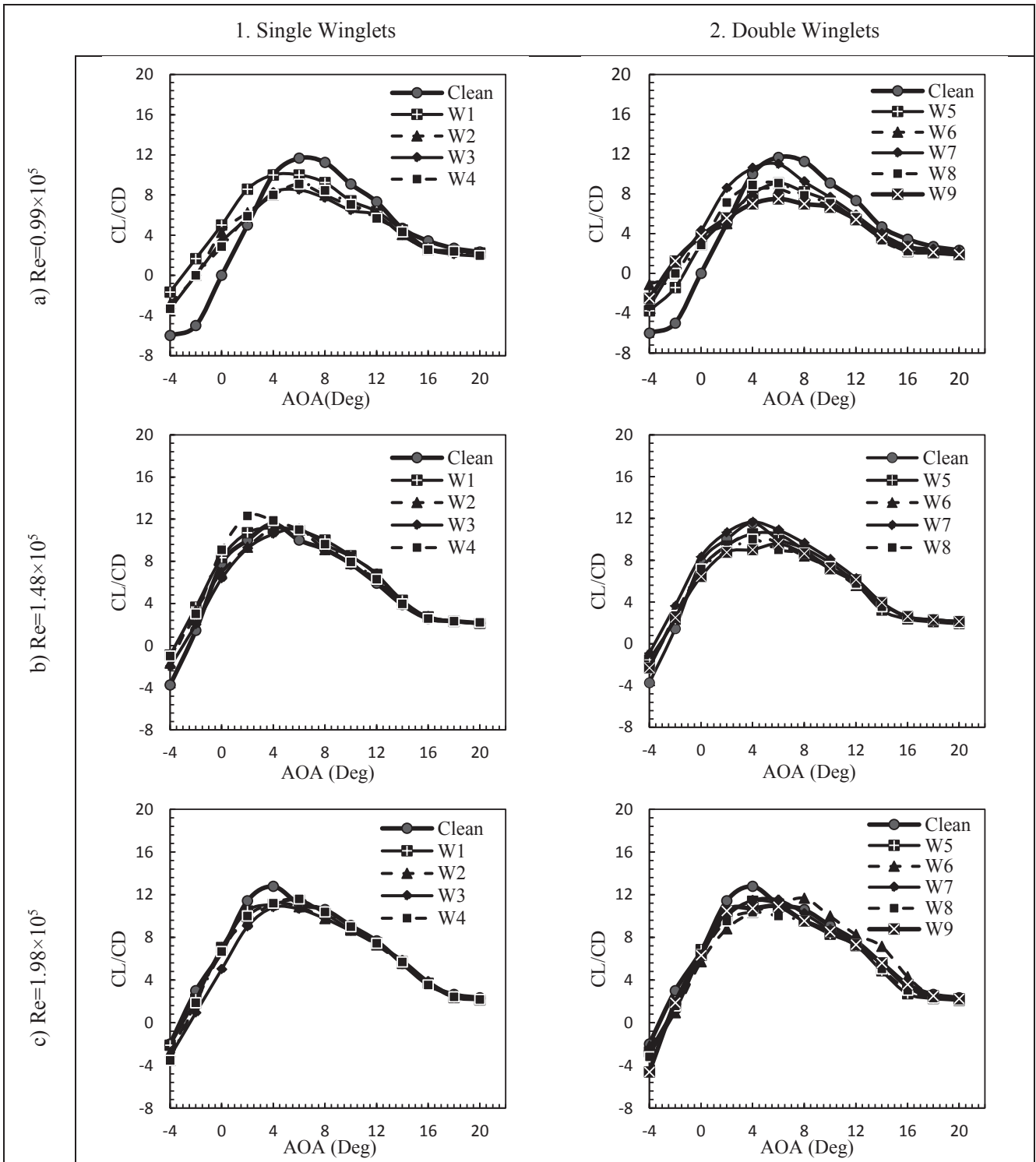
**Fig. 9. L/D versus angle of attack for wing with different winglets at different Reynolds numbers in two winglet planforms categories**

attack. It should be mentioned that at this Reynolds number, the maximum of *CL/CD* happened at AOA of 4°. the *CL/CD* related to the wing equipped with the W2 winglet represented a better performance at all angles of attack except at low angles of attack of 0° to 4°; also, the W3 winglet increased the *CL/CD* at negative angles and angles of attack higher than 4°. It should be noted that the W5, W8, and W9 winglets could improve the wing efficiency only at negative angles of attack; whereas the W6 winglet could improve the *CL/CD* of the wing at angles of attack higher than 4°, in addition to negative angles. W7 increased the wing efficiency at all angles of attack. There is not any considerable difference between the *CL/CD* of the winglets and the NACA $64_1412$. W6 showed a better performance compared to the base wing; however, in this Reynolds number, other winglets did not have any positive impact on the clean wing.

Studies presented in previous sections showed that winglet geometrical parameters influence the aerodynamic performance of a supercritical wing at a low Reynolds number greatly at a broad range of angles of attack. Among all these winglet models with different geometrical parameters, two models of W1 and W7 represented a significant enhancement of lift coefficient and lift-to-drag ratio; therefore, these two models are simulated numerically to figure out their effect on vortex drag reduction and wing tip vortices. In the subsequent paragraphs, the results obtained from this investigation will be expressed.

## 3- 3- Physics of Flow

For a better understanding of the physics of flow and to find the impact of each top-performance winglet planform on the flow phenomena, the contours of the vorticity and flow pattern are presented in Fig. 10 and Fig. 11. These contours are plotted for the base wing, wing equipped with W1 and W7 winglets for four different angles of attack of 0°, 4°, 8°, and 12° based on the fact that these two configurations represented the greatest improvements in aerodynamic efficiency. Admittedly, that the wing tip vortices play a critically important role in increasing the lift-induced drag is an undeniable fact; consequently, the vortices' size and strength could have a direct effect on the induced drag through the range of angles of attack.

The vorticity magnitude figures show that wing tip vortices for two winglet configurations and different angles of attack are distinct in their structure characteristics and strength formation. Generally, the vorticity magnitude is high near the trailing edge and diminishes at further locations; also, by increasing the angle of attack, the vorticity magnitude increases substantially. By paying attention to the base wing physics in different angles of attack, it could be understood that by the increment of the angle of attack, the wingtip vortices' size and magnitude corresponding to the strength of vortices are increased. This increment of wingtip vortice strength verifies the higher induced drag in previous experimental results. Also, by increment of the angle of attack, the length for flow to damp the tip vortices is increased corresponding to the lower impact of the aircraft

wingtip vortices on the aircraft located in the airport, which is one of the most common reasons for accidents due to tip vortices effects [36].

In addition, it can be seen from contours of the Fig. 10 and Fig. 11, that the vorticity magnitude of the wing models equipped with winglets is reduced noticeably, moved outboard and upward, and the cases for the wing equipped with winglets have smaller vortices formed at the tip. Therefore, it can be concluded that the winglets harness the energy of the tip vortex, leading to an enhanced aerodynamic efficiency, which is also proved through Fig. 9. As expected, winglets reduce the main wing-tip vortex intensity and create weaker vortices at the tips of the wings. To elaborate, these contours indicate that each model produces its individual vortices, which are much lower than the clean wing.

Furthermore, considering the contours of vorticity related to the W1 winglet, it can be observed that it improved the performance of the wing substantially in response to two factors, first, by attaching the W1 winglet to the clean wing, the intensity of the vorticity has been reduced to a great extent; also, wing tip vortices have been dissipated within the wake of the wing faster than the baseline wing. These findings align perfectly with the results found in previous sections representing that the W1 winglet improved the performance of the wing considerably. These explanations are also the same for the W7 winglet but with a slight difference that using double winglets resulted in both the upper and lower surface of the wing and it represented a higher performance improvement due to the fact that double winglets can prevent wingtip vortex formation and movement at two steps; lower and upper surface of the wing.

In sum, for both cases, the intensity of the main tip vortex is reduced, and two less-intense vortices are created at the tip of each planform. All these findings resulting from studying the physics of the flow confirm the results, which were previously obtained in terms of aerodynamic coefficients. For the W1 winglet, a short distance downstream of the wing, the vortices roll up and combine into two distinct cylindrical vortices that constitute the "tip vortices." These vortices trail back from the wing tips and they have a tendency to sink and roll toward each other downstream of the wing. Again, eventually, the tip vortices dissipate, their energy being transformed by viscosity.

## 4- Conclusion

Wingtip vortices are extremely important phenomena in fluid dynamics for their adverse effects in many applications. Therefore, in this paper, nine diverse winglets have been designed and tested experimentally and numerically at lower Reynolds numbers (take-off and landing phase of flight) to first, improve the performance of supercritical wings at this regime and second, study the influence of winglet geometrical parameters on controlling wingtip vortices. These tests were performed at a wide range of angles of attack and different Reynolds numbers to ensure that all the operational states were investigated. The results related to the variation of aerodynamic coefficients have been obtained
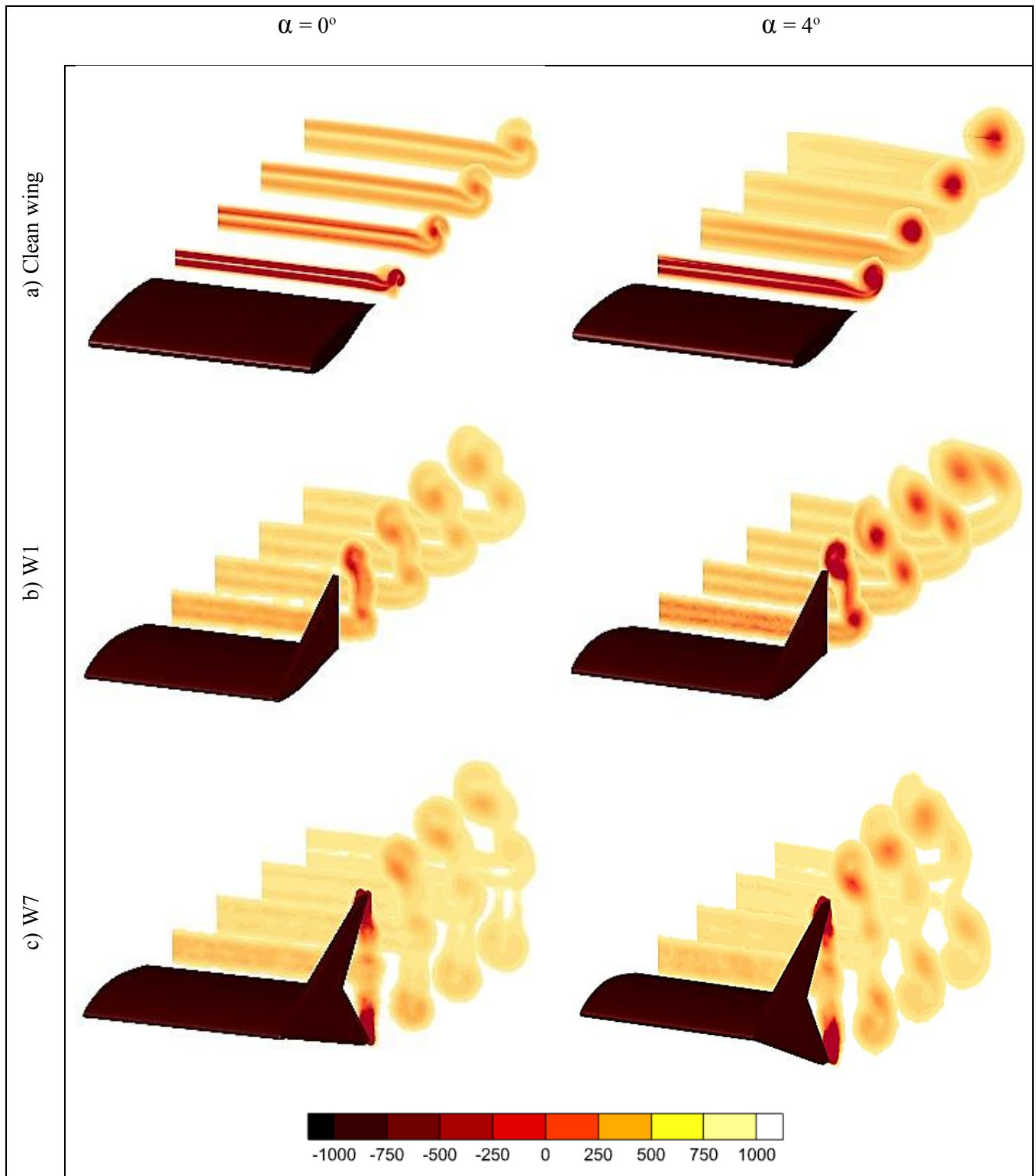
**Fig. 10. Vorticity magnitude contour for clean wing, W1 and W7 at α = 0° and α = 4°**

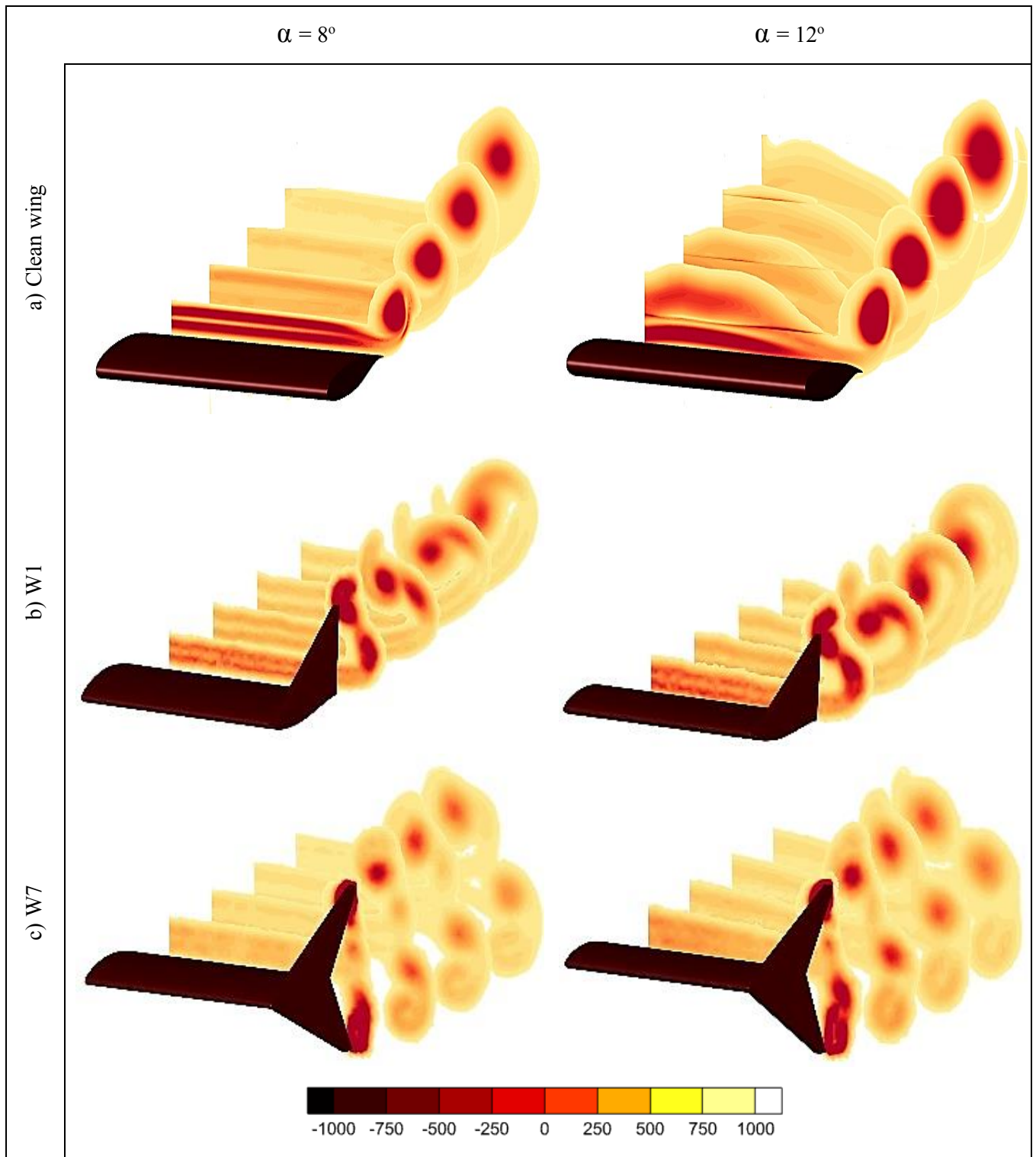**Fig. 11. Vorticity magnitude contour for clean wing, W1 and W7 at α = 0º and α = 4º**

through balance measurement, as well as the results related to vorticity magnitude for two models of W1 and W7. According to the results, various winglets with different geometrical parameters represented a great influence on the performance parameters of a supercritical wing at low Reynolds numbers. These results can be summarized below:

To begin with, all winglets increased the aerodynamic coefficients of a wing, such as $CL_{\alpha<0}$ (lift coefficient at negative angles of attack), $CL_o$, and $CL_a$. Also, from a stall behavior point of view, adding a winglet caused the wing to stall earlier at a lower angle of attack.

The first stage of the present study focused on the comparison of the lift coefficient of various winglet planforms against the baseline design. W1 winglet model has the most lift coefficient increment by 26% at its maximum for all Reynolds numbers; however, the percentage of this increment reduces as the Reynolds number increases. In contrast to the W1 model, the W3 winglet model showed the minimum lift increment. In addition, making the winglets with slanted height was not preferable because they did not represent any noticeable effect on the lift coefficient.

In the case of double winglets, for all winglets, except for W5, the double version of the winglets showed better performance compared to their single versions in terms of lift increment. Nevertheless, to differentiate these double winglets from their single forms and better identify them, it was required to assess the effect of these winglet models on other aerodynamic parameters of the wing, such as lift-to-drag ratio.

As previously mentioned, the best aerodynamic parameter for determining the viability of the used winglet model is the lift-to-drag ratio. Studying the figures related to this parameter revealed that the angle, at which maximum $CL/CD$ occurred remained the same as 6o for both clean wing and wing equipped with winglets. Regarding lift-to-drag ratio, the W1 winglet model showed the best performance up to 4o, and W7 was the best through a wide range of angles of attack.

In sum, the W7 winglet outperformed at increasing wing performance by 40% compared to other winglet models, and this effect was illustrated once again by the effect of this winglet model on wing tip vortices by reducing the vorticity magnitude significantly and changed the strong vortex of the clean wing into two weak vortices, which led to a remarkable performance enhancement of the considered wing.

## 5- Nomenclature

| | |
|---|---|
| $C_D$ | Drag coefficient of the wing |
| $C_L$ | Lift coefficient of the wing |
| $C_L/C_D$ | Lift to drag ratio |
| $V$ | Air free stream velocity (m/s) |
| $\alpha$ | Angle of attack (deg) |
| $CL_E$ | Lift Coefficient-Experimental |
| $CL_N$ | Lift Coefficient-Numerical |

Statements and Declarations

The authors declare no potential conflicts of interest with respect to the research, authorship, and/or publication of this article.

## References

[1] J.P. Eguea, G.P.G. da Silva, F.M. Catalano, Fuel efficiency improvement on a business jet using a camber morphing winglet concept, Aerospace Science and Technology, 96 (2020) 105542.

[2] M.A. Hasan, A.A. Mamun, S.M. Rahman, K. Malik, M.I.U. Al Amran, A.N. Khondaker, O. Reshi, S.P. Tiwari, F.S. Alismail, Climate change mitigation pathways for the aviation sector, Sustainability, 13(7) (2021) 3656.

[3] D.M. Bushnell, Aircraft drag reduction—a review, Proceedings of the Institution of Mechanical Engineers, Part G: Journal of Aerospace Engineering, 217(1) (2003) 1-18.

[4] J. Spillman, Wing tip sails; progress to date and future developments, The Aeronautical Journal, 91(910) (1987) 445-453.

[5] R.T. Whitcomb, A design approach and selected wind tunnel results at high subsonic speeds for wing-tip mounted winglets, 1976.

[6] M.D. Maughmer, T.S. Swan, S.M. Willits, Design and testing of a winglet airfoil for low-speed aircraft, Journal of Aircraft, 39(4) (2002) 654-661.

[7] A. Hossain, A. Rahman, A. Iqbal, M. Ariffin, M. Mazian, Drag analysis of an aircraft wing model with and without bird feather like winglet, International Journal of Aerospace and Mechanical Engineering, 6(1) (2012) 8-13.

[8] S. Kolappan, I.N. Manickam, K.R.J. Swikker, S.J.P. Gnanaraj, M. Appadurai, Performance analysis of aircraft composite winglet, Materials Today: Proceedings, 62 (2022) 889-895.

[9] M.T. Lewthwaite, C.V. Amaechi, Numerical investigation of winglet aerodynamics and dimple effect of NACA 0017 airfoil for a freight aircraft, Inventions, 7(1) (2022) 31.

[10] T. Seshaiah, B. Vasu, K.V.K. Reddy, P. Bridjesh, Analysis on air craft winglet at different angles by using CFD simulation, Materials today: Proceedings, 49 (2022) 275-283.

[11] M. Smith, N. Komerath, R. Ames, O. Wong, J. Pearson, Performance analysis of a wing with multiple winglets, in: 19th AIAA Applied Aerodynamics Conference, 2001, pp. 2407.

[12] J.P.L.G.M. Barrios, G.M.P. Herman, Reducing drag by modifying the winglet design, The Philippine Physics Society Physics Fair, Cebu. ResearchGate, (2017).

[13] S. Mousazadeh, M. Shahmardan, T. Tavangar, K. Hosseinzadeh, D. Ganji, Numerical investigation on convective heat transfer over two heated wall-mounted cubes in tandem and staggered arrangement, Theoretical and Applied Mechanics Letters, 8(3) (2018) 171-183.

[14] B. Mattos, A. Macedo, D. Silva Filho, Considerations about winglet design, in: 21st AIAA applied aerodynamics conference, 2003, pp. 3502.

[15] K.A. Al Sidairi, G. Rameshkumar, Design of winglet device for aircraft, International Journal of Multidisciplinary Sciences and Engineering, 7(1) (2016).

[16] G. Narayan, B. John, Effect of winglets induced tip vortex structure on the performance of subsonic wings, Aerospace Science and Technology, 58 (2016) 328-340.

[17] H. Helal, E.E. Khalil, O.E. Abdellatif, G.M. Elhariry, Aerodynamic Analyses of Aircraft-Blended Winglet Performance, IOSR J. Mech. Civ. Eng. Ver, 13(3) (2016) 2320-2334.

[18] R. Cosin, F.M. Catalano, L.G.N. Correa, R.M.U. Entz, Aerodynamic analysis of multi-winglets for low speed aircraft, in: 27th International congress of the aeronautical sciences, 2010, pp. 1622-1631.

[19] M.A. Azlin, C.M. Taib, S. Kasolang, F. Muhammad, CFD analysis of winglets at low subsonic flow, in: Proceedings of the World Congress on Engineering, 2011, pp. 6-8.

[20] S. Rajendran, Design of Parametric Winglets and Wing tip devices: A conceptual design approach, in, 2012.

[21] R. Nandi, M. Assad-Uz-Zaman, M.F. Rabbi, M. Mashud, Experimental Investigation of an Aircraft Wing Model Using Slotted Winglet, in, IEEE, 2014.

[22] S. Mostafa, S. Bose, A. Nair, M.A. Raheem, T. Majeed, A. Mohammed, Y. Kim, A parametric investigation of non-circular spiroid winglets, in: EPJ Web of Conferences, EDP Sciences, 2014, pp. 02077.

[23] P. Pragati, S. Baskar, Aerodynamic analysis of blended winglet for low speed aircraft, in: Proceedings of the World Congress on Engineering, 2015.

[24] N.N. Gavrilović, B.P. Rašuo, G.S. Dulikravich, V.B. Parezanović, Commercial aircraft performance improvement using winglets, FME Transactions, 43(1)

(2015) 1-8.

[25] I. Dimino, G. Andreutti, F. Moens, F. Fonte, R. Pecora, A. Concilio, Integrated design of a morphing winglet for active load control and alleviation of turboprop regional aircraft, Applied Sciences, 11(5) (2021) 2439.

[26] J. Zhong, W. Wu, S. Han, Research progress of tip winglet technology in compressor, Journal of Thermal Science, 30 (2021) 18-31.

[27] L.C. Montoya, S.G. Flechner, P.F. Jacobs, Effect of an alternate winglet on the pressure and spanwise load distributions of a first generation jet transport wing, 1978.

[28] S.B. MNVS, S.K.G. Kalali, B.N. Goud, A.S. Kumar, M.S. Gupta, Flow investigation of a multiple winglet wing model, in: AIP Conference Proceedings, AIP Publishing, 2023.

[29] K. Takenaka, K. Hatanaka, W. Yamazaki, K. Nakahashi, Multidisciplinary design exploration for a winglet, Journal of aircraft, 45(5) (2008) 1601-1611.

[30] J. Masud, Z. Toor, Z. Abbas, U. Ahsun, Part I: Uncertainty analysis of various design parameters on winglet performance, in: 54th AIAA Aerospace Sciences Meeting, 2016, pp. 0556.

[31] M.H. Sohn, J.W. Chang, Visualization and PIV study of wing-tip vortices for three different tip configurations, Aerospace Science and Technology, 16(1) (2012) 40-46.

[32] M. Ilie, M. White, V. Soloiu, M. Rahman, The effect of winglets on the aircraft wing aerodynamics; numerical studies using LES, in: AIAA Scitech 2019 Forum, 2019, pp. 1308.

[33] M.G. Mourad, I. Shahin, S.S. Ayad, O.E. Abdellatif, T.A. Mekhail, Effect of winglet geometry on horizontal axis wind turbine performance, Engineering reports, 2(1) (2020) e12101.

[34] F.J. Martinez Lara, D. Angland, The Use of Porous Meshes to Reduce Landing Gear Wake-Flap Interaction Noise, in: 28th AIAA/CEAS Aeroacoustics 2022 Conference, 2022, pp. 3044.

[35] F.R. Menter, Two-equation eddy-viscosity turbulence models for engineering applications, AIAA journal, 32(8) (1994) 1598-1605.

[36] R. Nelson, The trailing vortex wake hazard: Beyond the takeoff and landing corridors, in: AIAA Atmospheric Flight Mechanics Conference and Exhibit, 2004, pp. 5171.